Search for Scalar Top Quark Production in $p\bar{p}$ Collisions at $\sqrt{s} = 1.96$ TeV

T. Aaltonen,[21] B. Álvarez González[z],[9] S. Amerio,[40] D. Amidei,[32] A. Anastassov[x],[15] A. Annovi,[17] J. Antos,[12] G. Apollinari,[15] J.A. Appel,[15] T. Arisawa,[54] A. Artikov,[13] J. Asaadi,[49] W. Ashmanskas,[15] B. Auerbach,[57] A. Aurisano,[49] F. Azfar,[39] W. Badgett,[15] T. Bae,[25] A. Barbaro-Galtieri,[26] V.E. Barnes,[44] B.A. Barnett,[23] P. Barria[hh],[42] P. Bartos,[12] M. Bauce[ff],[40] F. Bedeschi,[42] S. Behari,[23] G. Bellettini[gg],[42] J. Bellinger,[56] D. Benjamin,[14] A. Beretvas,[15] A. Bhatti,[46] D. Bisello[ff],[40] I. Bizjak,[28] K.R. Bland,[5] B. Blumenfeld,[23] A. Bocci,[14] A. Bodek,[45] D. Bortoletto,[44] J. Boudreau,[43] A. Boveia,[11] L. Brigliadori[ee],[6] C. Bromberg,[33] E. Brucken,[21] J. Budagov,[13] H.S. Budd,[45] K. Burkett,[15] G. Busetto[ff],[40] P. Bussey,[19] A. Buzatu,[31] A. Calamba,[10] C. Calancha,[29] S. Camarda,[4] M. Campanelli,[28] M. Campbell,[32] F. Canelli[11],[15] B. Carls,[22] D. Carlsmith,[56] R. Carosi,[42] S. Carrillo[m],[16] S. Carron,[15] B. Casal[k],[9] M. Casarsa,[50] A. Castro[ee],[6] P. Catastini,[20] D. Cauz,[50] V. Cavaliere,[22] M. Cavalli-Sforza,[4] A. Cerri[f],[26] L. Cerrito[s],[28] Y.C. Chen,[1] M. Chertok,[7] G. Chiarelli,[42] G. Chlachidze,[15] F. Chlebana,[15] K. Cho,[25] D. Chokheli,[13] W.H. Chung,[56] Y.S. Chung,[45] M.A. Ciocci[hh],[42] A. Clark,[18] C. Clarke,[55] G. Compostella[ff],[40] M.E. Convery,[15] J. Conway,[7] M.Corbo,[15] M. Cordelli,[17] C.A. Cox,[7] D.J. Cox,[7] F. Crescioli[gg],[42] J. Cuevas[z],[9] R. Culbertson,[15] D. Dagenhart,[15] N. d'Ascenzo[w],[15] M. Datta,[15] P. de Barbaro,[45] M. Dell'Orso[gg],[42] L. Demortier,[46] M. Deninno,[6] F. Devoto,[21] M. d'Errico[ff],[40] A. Di Canto[gg],[42] B. Di Ruzza,[15] J.R. Dittmann,[5] M. D'Onofrio,[27] S. Donati[gg],[42] P. Dong,[15] M. Dorigo,[50] T. Dorigo,[40] K. Ebina,[54] A. Elagin,[49] A. Eppig,[32] R. Erbacher,[7] S. Errede,[22] N. Ershaidat[dd],[15] R. Eusebi,[49] S. Farrington,[39] M. Feindt,[24] J.P. Fernandez,[29] R. Field,[16] G. Flanagan[u],[15] R. Forrest,[7] M.J. Frank,[5] M. Franklin,[20] J.C. Freeman,[15] Y. Funakoshi,[54] I. Furic,[16] M. Gallinaro,[46] J.E. Garcia,[18] A.F. Garfinkel,[44] P. Garosi[hh],[42] H. Gerberich,[22] E. Gerchtein,[15] S. Giagu,[47] V. Giakoumopoulou,[3] P. Giannetti,[42] K. Gibson,[43] C.M. Ginsburg,[15] N. Giokaris,[3] P. Giromini,[17] G. Giurgiu,[23] V. Glagolev,[13] D. Glenzinski,[15] M. Gold,[35] D. Goldin,[49] N. Goldschmidt,[16] A. Golossanov,[15] G. Gomez,[9] G. Gomez-Ceballos,[30] M. Goncharov,[30] O. González,[29] I. Gorelov,[35] A.T. Goshaw,[14] K. Goulianos,[46] S. Grinstein,[4] C. Grosso-Pilcher,[11] R.C. Group[53],[15] J. Guimaraes da Costa,[20] S.R. Hahn,[15] E. Halkiadakis,[48] A. Hamaguchi,[38] J.Y. Han,[45] F. Happacher,[17] K. Hara,[51] D. Hare,[48] M. Hare,[52] R.F. Harr,[55] K. Hatakeyama,[5] C. Hays,[39] M. Heck,[24] J. Heinrich,[41] M. Herndon,[56] S. Hewamanage,[5] A. Hocker,[15] W. Hopkins[g],[15] D. Horn,[24] S. Hou,[1] R.E. Hughes,[36] M. Hurwitz,[11] U. Husemann,[57] N. Hussain,[31] M. Hussein,[33] J. Huston,[33] G. Introzzi,[42] M. Iori[jj],[47] A. Ivanov[p],[7] E. James,[15] D. Jang,[10] B. Jayatilaka,[14] E.J. Jeon,[25] S. Jindariani,[15] M. Jones,[44] K.K. Joo,[25] S.Y. Jun,[10] T.R. Junk,[15] T. Kamon[25],[49] P.E. Karchin,[55] A. Kasmi,[5] Y. Kato[o],[38] W. Ketchum,[11] J. Keung,[41] V. Khotilovich,[49] B. Kilminster,[15] D.H. Kim,[25] H.S. Kim,[25] J.E. Kim,[25] M.J. Kim,[17] S.B. Kim,[25] S.H. Kim,[51] Y.K. Kim,[11] Y.J. Kim,[25] N. Kimura,[54] M. Kirby,[15] S. Klimenko,[16] K. Knoepfel,[15] K. Kondo*,[54] D.J. Kong,[25] J. Konigsberg,[16] A.V. Kotwal,[14] M. Kreps,[24] J. Kroll,[41] D. Krop,[11] M. Kruse,[14] V. Krutelyov[c],[49] T. Kuhr,[24] M. Kurata,[51] S. Kwang,[11] A.T. Laasanen,[44] S. Lami,[42] S. Lammel,[15] M. Lancaster,[28] R.L. Lander,[7] K. Lannon[y],[36] A. Lath,[48] G. Latino[hh],[42] T. LeCompte,[2] E. Lee,[49] H.S. Lee[q],[11] J.S. Lee,[25] S.W. Lee[bb],[49] S. Leo[gg],[42] S. Leone,[42] J.D. Lewis,[15] A. Limosani[t],[14] C.-J. Lin,[26] M. Lindgren,[15] E. Lipeles,[41] A. Lister,[18] D.O. Litvintsev,[15] C. Liu,[43] H. Liu,[53] Q. Liu,[44] T. Liu,[15] S. Lockwitz,[57] A. Loginov,[57] D. Lucchesi[ff],[40] J. Lueck,[24] P. Lujan,[26] P. Lukens,[15] G. Lungu,[46] J. Lys,[26] R. Lysak[e],[12] R. Madrak,[15] K. Maeshima,[15] P. Maestro[hh],[42] S. Malik,[46] G. Manca[a],[27] A. Manousakis-Katsikakis,[3] F. Margaroli,[47] C. Marino,[24] M. Martínez,[4] P. Mastrandrea,[47] K. Matera,[22] M.E. Mattson,[55] A. Mazzacane,[15] P. Mazzanti,[6] K.S. McFarland,[45] P. McIntyre,[49] R. McNulty[j],[27] A. Mehta,[27] P. Mehtala,[21] C. Mesropian,[46] T. Miao,[15] D. Mietlicki,[32] A. Mitra,[1] H. Miyake,[51] S. Moed,[15] N. Moggi,[6] M.N. Mondragon[m],[15] C.S. Moon,[25] R. Moore,[15] M.J. Morello[ii],[42] J. Morlock,[24] P. Movilla Fernandez,[15] A. Mukherjee,[15] Th. Muller,[24] P. Murat,[15] M. Mussini[ee],[6] J. Nachtman[n],[15] Y. Nagai,[51] J. Naganoma,[54] I. Nakano,[37] A. Napier,[52] J. Nett,[49] C. Neu,[53] M.S. Neubauer,[22] J. Nielsen[d],[26] L. Nodulman,[2] S.Y. Noh,[25] O. Norniella,[22] L. Oakes,[39] S.H. Oh,[14] Y.D. Oh,[25] I. Oksuzian,[53] T. Okusawa,[38] R. Orava,[21] L. Ortolan,[4] S. Pagan Griso[ff],[40] C. Pagliarone,[50] E. Palencia[f],[9] V. Papadimitriou,[15] A.A. Paramonov,[2] J. Patrick,[15] G. Pauletta[kk],[50] M. Paulini,[10] C. Paus,[30] D.E. Pellett,[7] A. Penzo,[50] T.J. Phillips,[14] G. Piacentino,[42] E. Pianori,[41] J. Pilot,[36] K. Pitts,[22] C. Plager,[8] L. Pondrom,[56] S. Poprocki[g],[15] K. Potamianos,[44] F. Prokoshin[cc],[13] A. Pranko,[26] F. Ptohos[h],[17] G. Punzi[gg],[42] A. Rahaman,[43] V. Ramakrishnan,[56] N. Ranjan,[44] I. Redondo,[29] P. Renton,[39] M. Rescigno,[47] T. Riddick,[28] F. Rimondi[ee],[6] L. Ristori[42],[15] A. Robson,[19] T. Rodrigo,[9] T. Rodriguez,[41] E. Rogers,[22] S. Rolli[i],[52] R. Roser,[15] F. Ruffini[hh],[42] A. Ruiz,[9] J. Russ,[10] V. Rusu,[15] A. Safonov,[49] W.K. Sakumoto,[45] Y. Sakurai,[54] L. Santi[kk],[50] K. Sato,[51] V. Saveliev[w],[15] A. Savoy-Navarro[aa],[15] P. Schlabach,[15] A. Schmidt,[24] E.E. Schmidt,[15] T. Schwarz,[15] L. Scodellaro,[9] A. Scribano[hh],[42] F. Scuri,[42] S. Seidel,[35] Y. Seiya,[38] A. Semenov,[13] F. Sforza[hh],[42] S.Z. Shalhout,[7] T. Shears,[27]

P.F. Shepard,[43] M. Shimojima[v],[51] M. Shochet,[11] I. Shreyber-Tecker,[34] A. Simonenko,[13] P. Sinervo,[31] K. Sliwa,[52] J.R. Smith,[7] F.D. Snider,[15] A. Soha,[15] V. Sorin,[4] H. Song,[43] P. Squillacioti[hh],[42] M. Stancari,[15] R. St. Denis,[19] B. Stelzer,[31] O. Stelzer-Chilton,[31] D. Stentz[x],[15] J. Strologas,[35] G.L. Strycker,[32] Y. Sudo,[51] A. Sukhanov,[15] I. Suslov,[13] K. Takemasa,[51] Y. Takeuchi,[51] J. Tang,[11] M. Tecchio,[32] P.K. Teng,[1] J. Thom[g],[15] J. Thome,[10] G.A. Thompson,[22] E. Thomson,[41] D. Toback,[49] S. Tokar,[12] K. Tollefson,[33] T. Tomura,[51] D. Tonelli,[15] S. Torre,[17] D. Torretta,[15] P. Totaro,[40] M. Trovato[ii],[42] F. Ukegawa,[51] S. Uozumi,[25] A. Varganov,[32] F. Vázquez[m],[16] G. Velev,[15] C. Vellidis,[15] M. Vidal,[44] I. Vila,[9] R. Vilar,[9] J. Vizán,[9] M. Vogel,[35] G. Volpi,[17] P. Wagner,[41] R.L. Wagner,[15] T. Wakisaka,[38] R. Wallny,[8] S.M. Wang,[1] A. Warburton,[31] D. Waters,[28] W.C. Wester III,[15] D. Whiteson[b],[41] A.B. Wicklund,[2] E. Wicklund,[15] S. Wilbur,[11] F. Wick,[24] H.H. Williams,[41] J.S. Wilson,[36] P. Wilson,[15] B.L. Winer,[36] P. Wittich[g],[15] S. Wolbers,[15] H. Wolfe,[36] T. Wright,[32] X. Wu,[18] Z. Wu,[5] K. Yamamoto,[38] D. Yamato,[38] T. Yang,[15] U.K. Yang[r],[11] Y.C. Yang,[25] W.-M. Yao,[26] G.P. Yeh,[15] K. Yi[n],[15] J. Yoh,[15] K. Yorita,[54] T. Yoshida[l],[38] G.B. Yu,[14] I. Yu,[25] S.S. Yu,[15] J.C. Yun,[15] A. Zanetti,[50] Y. Zeng,[14] C. Zhou,[14] and S. Zucchelli[ee][6]

(CDF Collaboration[†])

[1]Institute of Physics, Academia Sinica, Taipei, Taiwan 11529, Republic of China
[2]Argonne National Laboratory, Argonne, Illinois 60439, USA
[3]University of Athens, 157 71 Athens, Greece
[4]Institut de Fisica d'Altes Energies, ICREA, Universitat Autonoma de Barcelona, E-08193, Bellaterra (Barcelona), Spain
[5]Baylor University, Waco, Texas 76798, USA
[6]Istituto Nazionale di Fisica Nucleare Bologna, [ee]University of Bologna, I-40127 Bologna, Italy
[7]University of California, Davis, Davis, California 95616, USA
[8]University of California, Los Angeles, Los Angeles, California 90024, USA
[9]Instituto de Fisica de Cantabria, CSIC-University of Cantabria, 39005 Santander, Spain
[10]Carnegie Mellon University, Pittsburgh, Pennsylvania 15213, USA
[11]Enrico Fermi Institute, University of Chicago, Chicago, Illinois 60637, USA
[12]Comenius University, 842 48 Bratislava, Slovakia; Institute of Experimental Physics, 040 01 Kosice, Slovakia
[13]Joint Institute for Nuclear Research, RU-141980 Dubna, Russia
[14]Duke University, Durham, North Carolina 27708, USA
[15]Fermi National Accelerator Laboratory, Batavia, Illinois 60510, USA
[16]University of Florida, Gainesville, Florida 32611, USA
[17]Laboratori Nazionali di Frascati, Istituto Nazionale di Fisica Nucleare, I-00044 Frascati, Italy
[18]University of Geneva, CH-1211 Geneva 4, Switzerland
[19]Glasgow University, Glasgow G12 8QQ, United Kingdom
[20]Harvard University, Cambridge, Massachusetts 02138, USA
[21]Division of High Energy Physics, Department of Physics,
University of Helsinki and Helsinki Institute of Physics, FIN-00014, Helsinki, Finland
[22]University of Illinois, Urbana, Illinois 61801, USA
[23]The Johns Hopkins University, Baltimore, Maryland 21218, USA
[24]Institut für Experimentelle Kernphysik, Karlsruhe Institute of Technology, D-76131 Karlsruhe, Germany
[25]Center for High Energy Physics: Kyungpook National University,
Daegu 702-701, Korea; Seoul National University, Seoul 151-742,
Korea; Sungkyunkwan University, Suwon 440-746,
Korea; Korea Institute of Science and Technology Information,
Daejeon 305-806, Korea; Chonnam National University, Gwangju 500-757,
Korea; Chonbuk National University, Jeonju 561-756, Korea
[26]Ernest Orlando Lawrence Berkeley National Laboratory, Berkeley, California 94720, USA
[27]University of Liverpool, Liverpool L69 7ZE, United Kingdom
[28]University College London, London WC1E 6BT, United Kingdom
[29]Centro de Investigaciones Energeticas Medioambientales y Tecnologicas, E-28040 Madrid, Spain
[30]Massachusetts Institute of Technology, Cambridge, Massachusetts 02139, USA
[31]Institute of Particle Physics: McGill University, Montréal, Québec,
Canada H3A 2T8; Simon Fraser University, Burnaby, British Columbia,
Canada V5A 1S6; University of Toronto, Toronto, Ontario,
Canada M5S 1A7; and TRIUMF, Vancouver, British Columbia, Canada V6T 2A3
[32]University of Michigan, Ann Arbor, Michigan 48109, USA
[33]Michigan State University, East Lansing, Michigan 48824, USA
[34]Institution for Theoretical and Experimental Physics, ITEP, Moscow 117259, Russia
[35]University of New Mexico, Albuquerque, New Mexico 87131, USA
[36]The Ohio State University, Columbus, Ohio 43210, USA
[37]Okayama University, Okayama 700-8530, Japan
[38]Osaka City University, Osaka 588, Japan

[39] University of Oxford, Oxford OX1 3RH, United Kingdom
[40] Istituto Nazionale di Fisica Nucleare, Sezione di Padova-Trento, [ff] University of Padova, I-35131 Padova, Italy
[41] University of Pennsylvania, Philadelphia, Pennsylvania 19104, USA
[42] Istituto Nazionale di Fisica Nucleare Pisa, [gg] University of Pisa,
[hh] University of Siena and [ii] Scuola Normale Superiore, I-56127 Pisa, Italy
[43] University of Pittsburgh, Pittsburgh, Pennsylvania 15260, USA
[44] Purdue University, West Lafayette, Indiana 47907, USA
[45] University of Rochester, Rochester, New York 14627, USA
[46] The Rockefeller University, New York, New York 10065, USA
[47] Istituto Nazionale di Fisica Nucleare, Sezione di Roma 1,
[jj] Sapienza Università di Roma, I-00185 Roma, Italy
[48] Rutgers University, Piscataway, New Jersey 08855, USA
[49] Texas A&M University, College Station, Texas 77843, USA
[50] Istituto Nazionale di Fisica Nucleare Trieste/Udine,
I-34100 Trieste, [kk] University of Udine, I-33100 Udine, Italy
[51] University of Tsukuba, Tsukuba, Ibaraki 305, Japan
[52] Tufts University, Medford, Massachusetts 02155, USA
[53] University of Virginia, Charlottesville, Virginia 22906, USA
[54] Waseda University, Tokyo 169, Japan
[55] Wayne State University, Detroit, Michigan 48201, USA
[56] University of Wisconsin, Madison, Wisconsin 53706, USA
[57] Yale University, New Haven, Connecticut 06520, USA
(Dated: March 19, 2012)

We report on a search for the supersymmetric partner of the top quark (scalar top) decaying into a charm quark and a neutralino in $p\bar{p}$ collisions at $\sqrt{s} = 1.96$ TeV. The data sample, collected by the CDF II detector at the Fermilab Tevatron, corresponds to an integrated luminosity of 2.6 fb^{-1}. Candidate events are selected by requiring two or more jets and a large imbalance in the transverse momentum. To enhance the analysis sensitivity, at least one of the jets is required to be identified as originating from a charm quark using an algorithm specifically designed for this analysis. The selected events are in good agreement with standard model predictions. In the case of large mass splitting between the scalar top quark and the neutralino we exclude a scalar top quark mass below 180 GeV/c^2 at 95% confidence level.

PACS numbers: 14.80.Ly

[*] Deceased
[†] With visitors from [a] Istituto Nazionale di Fisica Nucleare, Sezione di Cagliari, 09042 Monserrato (Cagliari), Italy, [b] University of CA Irvine, Irvine, CA 92697, USA, [c] University of CA Santa Barbara, Santa Barbara, CA 93106, USA, [d] University of CA Santa Cruz, Santa Cruz, CA 95064, USA, [e] Institute of Physics, Academy of Sciences of the Czech Republic, Czech Republic, [f] CERN, CH-1211 Geneva, Switzerland, [g] Cornell University, Ithaca, NY 14853, USA, [h] University of Cyprus, Nicosia CY-1678, Cyprus, [i] Office of Science, U.S. Department of Energy, Washington, DC 20585, USA, [j] University College Dublin, Dublin 4, Ireland, [k] ETH, 8092 Zurich, Switzerland, [l] University of Fukui, Fukui City, Fukui Prefecture, Japan 910-0017, [m] Universidad Iberoamericana, Mexico D.F., Mexico, [n] University of Iowa, Iowa City, IA 52242, USA, [o] Kinki University, Higashi-Osaka City, Japan 577-8502, [p] Kansas State University, Manhattan, KS 66506, USA, [q] Ewha Womans University, Seoul, 120-750, Korea, [r] University of Manchester, Manchester M13 9PL, United Kingdom, [s] Queen Mary, University of London, London, E1 4NS, United Kingdom, [t] University of Melbourne, Victoria 3010, Australia, [u] Muons, Inc., Batavia, IL 60510, USA, [v] Nagasaki Institute of Applied Science, Nagasaki, Japan, [w] National Research Nuclear University, Moscow, Russia, [x] Northwestern University, Evanston, IL 60208, USA, [y] University of Notre Dame, Notre Dame, IN 46556, USA, [z] Universidad de Oviedo, E-33007 Oviedo, Spain, [aa] CNRS-IN2P3, Paris, F-75205 France, [bb] Texas Tech University, Lubbock, TX 79609, USA, [cc] Universidad Tecnica Federico Santa Maria, 110v Valparaiso, Chile, [dd] Yarmouk University, Irbid 211-63, Jordan,

The standard model (SM) of elementary particles and fundamental interactions, however successful, is still incomplete since it does not explain the origin of electroweak symmetry breaking and does not give an answer to the gauge hierarchy problem [1]. A possible extension of the SM, supersymmetry (SUSY) [2], solves these problems by introducing a symmetry that relates particles of different spin. R-parity [2] conserving SUSY models also provide a prime candidate for the dark matter in the universe [3], namely the stable lightest supersymmetric particle (LSP). In these models, the left-handed and right-handed quarks have scalar partners, respectively denoted as $\tilde{q}_L$ and $\tilde{q}_R$, which can mix to form scalar quarks with mass eigenstates $\tilde{q}_{1,2}$. Several models [4] predict that this mixing can be substantial for the scalar top (stop), yielding a stop mass eigenstate ($\tilde{t}_1$) significantly lighter than other scalar quarks. If the $\tilde{t}_1$ is sufficiently light, it can be pair-produced copiously in proton-antiproton collisions at center-of-mass energy of $\sqrt{s} = 1.96$ TeV at

the Tevatron. A stop in the mass range accessible at the Tevatron is expected to decay predominantly into a charm quark and the lightest neutralino ($\tilde{\chi}_1^0$), which is often assumed to be the LSP. Assuming R-parity conservation, stops are produced in pairs. We consider a scenario where $m_{\tilde{t}_1} < m_b + m_{\tilde{\chi}^+}$ (where $\tilde{\chi}^+$ is a chargino), and $m_{\tilde{t}_1} < m_W + m_b + m_{\tilde{\chi}_1^0}$. Under these conditions the decay $\tilde{t}_1 \to c\tilde{\chi}_1^0$ is dominant. Results from searches using this final state at the Tevatron have been previously reported in [5, 6].

In this Letter, we report the search for $\tilde{t}_1 \to c\tilde{\chi}_1^0$ decays in $p\bar{p}$ collision data from 2.6 fb^{-1} of integrated luminosity collected by the upgraded Collider Detector at Fermilab (CDF II) at the Tevatron. The final state contains two c jets from the hadronization of the c quarks and features an imbalance in transverse momentum ("missing transverse energy" or $\not\!\!E_T$ [7]) from the two LSPs escaping detection.

CDF II is a multipurpose detector, described in detail elsewhere [8]. The charged-particle tracking system consists of silicon microstrip detectors and a cylindrical open-cell drift chamber, both of which are immersed in a 1.4 T solenoidal magnetic field coaxial with the beam line. The silicon detectors provide coverage in the pseudorapidity [7] range $|\eta| \leq 2$ and are used to identify events with long-lived particle decays. The drift chamber surrounds the silicon detectors, has maximum tracking efficiency up to $|\eta| = 1$, and is used for charged particle momentum measurements. Segmented sampling calorimeters, which surround the tracking system, are arranged in a projective tower geometry and are used to measure the energy of interacting particles in the region $|\eta| < 3.6$. Muon candidates are identified by drift chambers, which extend up to $|\eta| = 1.5$, and are located outside the calorimeter volume. Jets are reconstructed from the energy depositions in the calorimeter cells using an iterative cone jet-clustering algorithm [9], with a cone size of radius $R = \sqrt{(\Delta\phi)^2 + (\Delta\eta)^2} = 0.7$ [7]. Energy corrections [10] are applied to account for effects such as non-linear calorimeter response, underlying event, and the position of the interaction point, that influence the measured transverse jet energy.

Candidate events used for this search are selected by an online event selection system (trigger) that requires $\not\!\!E_T \geq$ 35 GeV and two jets. Further selections are applied offline to remove accelerator-produced and detector-related backgrounds as well as cosmic-ray events. After offline event reconstruction, the events are required to have $\not\!\!E_T \geq 50$ GeV, and at least two jets with $|\eta| \leq 2.4$ and $E_T \geq 25$ GeV. The highest-E_T jet is required to have $E_T \geq 35$ GeV and at least one of the selected jets is required to be in the region $|\eta| \leq 0.9$.

The hadrons in jets coming from b or c quark fragmentation, heavy-flavor (HF) jets, have a measurable flight path, yielding secondary vertices relative to the $p\bar{p}$ inter-

action point (primary vertex). We require the events to have exactly one jet identified as a HF jet by the secondary-vertex tagging algorithm [11], since requiring two HF-identified jets enhances the sample with events containing two b quarks and reduces the signal acceptance. This criteria defines a preselection which is used as the basis of background studies and further optimization for the signal sample, as described below.

Dominant SM backgrounds are pair and single top-quark production, electroweak single and di-boson production, HF multijet production, and light-flavor multijet events where one of the jets is falsely tagged as a HF jet (mistag). The latter two background contributions are estimated from data. The ALPGEN [12] event generator interfaced with the parton-shower model from the PYTHIA [13] event generator is used to estimate the electroweak boson production, the MADEVENT [14] generator is used to model the single top events, while the PYTHIA event generator is used to model the top-quark pair and diboson backgrounds. For the event generation the CTEQ5L [15] parton distribution functions (PDFs) are used. Simulated events are passed through the GEANT3-based [16] CDF II detector simulation [17] and are weighted by the probability that they would pass the trigger selection. The single top-quark and diboson contributions are normalized to the theoretical cross sections [18–20]. The contributions for the electroweak boson samples are normalized to the next-to-leading order cross sections calculated with MCFM [21]. We use the measured top-quark pair production cross section of $\sigma_{t\bar{t}} = 7.02 \pm 0.63$ pb [22]. Mistags are estimated based on the mistag rate [11] observed in inclusive jet data. The mistag rate is parametrized as a function of jet E_T, $|\eta|$, secondary-vertex track-multiplicity, the number of primary vertices in the event, primary vertex z-position, and the scalar sum of E_T of all jets in the event. To estimate the HF multijet background from data, we use a multijet tag rate estimator (MUTARE) described elsewhere [23, 24]. The HF multijet prediction from MUTARE is scaled by a multiplicative factor that is obtained in a signal-free region.

To avoid potential biases when searching for new physics, we test the various background contributions in distinct control regions that are defined *a priori*. The three control regions used to validate the SM prediction are denoted as multijet, lepton, and pre-optimization regions. The multijet control region is defined to have the second leading E_T jet direction ($\vec{j}_2$) aligned with the $\vec{\not\!\!E}_T$ [7], where aligned means $\Delta\phi(\vec{\not\!\!E}_T, \vec{j}_2) \leq 0.4$ rad. This HF multijet enriched region is used to obtain the MUTARE parameterization to predict the HF multijet background in the other control and signal regions. The lepton control region is defined to have $\vec{j}_2$ direction not aligned with the $\vec{\not\!\!E}_T$ ($\Delta\phi(\vec{\not\!\!E}_T, \vec{j}_2) \geq 0.7$ rad) and at least one isolated charged lepton (e or μ) with $p_T \geq 10$ GeV/c. This lepton region is used to validate the modeling of

TABLE I: Comparison of the total number of expected and observed events in the control regions. The total uncertainty is computed by taking into account the (anti)correlations between the partial uncertainties. In the lepton region the HF multijet prediction is scaled to match the observed events in order to perform shape comparisons only.

Regions:	Multijet	Lepton	Pre-optimization
W/Z + jets	457 ± 190	375 ± 156	1551 ± 644
Diboson	17 ± 2	45 ± 5	118 ± 13
Top pair	188 ± 21	547 ± 60	870 ± 96
Single top	11 ± 2	71 ± 10	130 ± 19
HF multijets	75407 ± 23376	268 ± 83	12935 ± 4010
Light-flavor jets	65839 ± 8427	720 ± 92	7741 ± 991
Total expected	141919 ± 24849	2026 ± 208	23345 ± 4182
Observed	143441	2026	22792

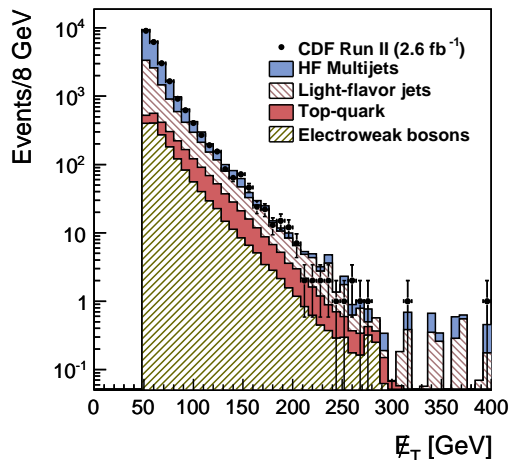FIG. 1: Distribution of $\displaystyle{\not}E_T$ in the pre-optimization region. SM prediction (stacked histograms) and observed distribution (dots) are shown, where HF multijets and light-flavor jets are predicted from data.

the top quark and electroweak W/Z boson backgrounds. The pre-optimization control region is defined to have the leading and second leading E_T jets not aligned with the $\overrightarrow{\not}E_T$ and to have no identified leptons. We studied kinematic distributions such as jet E_T, $\not{E}_T$, as well as the total numbers of events predicted. All these quantities are in agreement with observations in the three control regions. As an example, the $\not{E}_T$ distributions for the pre-optimization region are shown in Fig. 1. Table I presents the expected event yields for various background processes in the control regions under study.

We optimize the sensitivity to stop production by applying additional event selection criteria using a set of cuts suppressing the HF multijet background. We

select events with exactly two jets, as expected from the signal, and fulfilling the condition $\Delta\phi(\overrightarrow{\not}E_T, \overrightarrow{\not}E_T^{trk}) < \pi/2$. This variable is the angular difference between the calorimetry-based $\overrightarrow{\not}E_T$ and the same quantity calculated using tracks ($\overrightarrow{\not}E_T^{trk}$) [7]. When the $\not{E}_T$ in the event is real, these two quantities are usually aligned in ϕ. However, when the $\not{E}_T$ comes from calorimetry mis-measurements, as in HF multijet events with no real $\not{E}_T$, the angular difference between the two quantities is randomly distributed.

To further improve the sensitivity we apply a neural network (NN) trained with the TMVA package [25], to reduce the remaining HF multijet background. We train the NN using jet E_T, jet η, the minimum $\Delta\phi$ between the $\overrightarrow{\not}E_T$ and any of the selected jets, $\Delta\phi(\overrightarrow{\not}E_T, \overrightarrow{\not}E_T^{trk})$, $\Delta\phi(\vec{j}_1, \vec{j}_2)$, $\not{E}_T$, $\not{E}_T^{trk}$, and the summed E_T of all the jets in the event. We choose a reference signal point with $m(\tilde{t}_1) = 125$ GeV/c^2 and $m(\tilde{\chi}_1^0) = 70$ GeV/c^2 to perform the optimization. The signal acceptance is obtained using the PYTHIA event generator and CTEQ5L PDFs. Total signal yields are normalized to the NLO production cross section determined with the PROSPINO event generator [26] and the CTEQ6M [27, 28] PDFs. The uncertainty of the NLO production cross section is estimated to be 20%, arising from the scale dependence and the uncertainties on the PDFs. The NN output lies within -1 and 1, where the background peaks at -1 and the signal peaks at 1. We define our signal region as events with NN output scores > 0.

The final stage in the optimization is the application of a charm hadron analysis oriented separator (CHAOS) technique [24], explicitly designed for this analysis to obtain a sample enriched in c jets. CHAOS is a NN producing a two-dimensional output and trained with the SNNS v4.3 package [29] to determine whether a jet identified as HF has been produced from the hadronization process of a light quark falsely tagged as a HF jet, a b quark, or a c quark. The two-dimensional output structure allows the separation of the three different targets during the same training process. Depending on the flavor of the original parton, the jet identified as HF and its secondary vertex have different characteristics, mainly related to the tracking. Using properties of the tracks forming the secondary vertex and the tracks of the jets within a neural network, CHAOS allows enhancement of the jet selection with a desired flavor, in particular c jets. We apply CHAOS to the jet identified as HF and we find that the optimal cut has a selection efficiency [24] of 34% for c jets, 7.3% for b jets, and 4.9% for light jets.

The systematic uncertainties on the signal and the background predictions, taking into account correlated and uncorrelated uncertainties, are studied. Correlated uncertainties, affecting both the background prediction and signal acceptance, are dominated by the uncertainties on the performance of the b-tagging algorithm and

TABLE II: Number of expected and observed events in the signal region before and after CHAOS application. Prediction for the signal point $(m(\tilde{t}_1) = 125 \text{ GeV}/c^2$, $m(\tilde{\chi}_1^0) = 70 \text{ GeV}/c^2$) is also shown. Correlated and uncorrelated uncertainties in the total background and expected signal were treated separately in the analysis although they are combined here.

Signal region	Before CHAOS	Final (after CHAOS)
W/Z + jets	423.6 ± 185.0	60.9 ± 26.6
Diboson	36.9 ± 6.5	10.7 ± 1.9
Top pair	61.9 ± 15.5	4.6 ± 1.3
Single top	39.0 ± 9.7	3.2 ± 0.8
HF Multijets	279.6 ± 208.3	20.4 ± 15.2
Light-flavor jets	658.3 ± 259.6	32.2 ± 12.7
Total expected	1499.3 ± 277.1	132.0 ± 24.4
Observed	1496	115
$\tilde{t}_1$ signal	250.0 ± 66.2	90.2 ± 23.9

CHAOS, which are 4.4% [11] and 9.2% respectively, and the luminosity (6%) [8]. Uncorrelated systematic uncertainties on the background predictions are dominated by uncertainties on the MUTARE parameterization (30%), the mistag rate (16% [11] for light-flavor multijets), the top-quark pair-production cross section (11%), the single top-quark production cross section (13%), and the diboson production cross section (10% for WW/WZ and 20% for ZZ). The uncertainty on the normalization of the boson plus HF jets to the total inclusive boson production cross section translates into a 10% uncertainty in the SM predictions. Correlated and uncorrelated uncertainties are evaluated separately and combined in quadrature.

The signal region is analyzed after the background predictions are determined. We observe 115 events, where 132.0 ± 24.4 are expected from background, as summarized in Table II where yields before selecting events based on CHAOS output are also shown. Since no significant deviation from the SM prediction is observed, the results are used to calculate a 95% C.L. exclusion limit for the $\tilde{t}_1$ pair production cross section.

We have used the differences in shape of the NN output to set the limits. These limits are computed using a Bayesian likelihood method [31] with a flat prior probability for the signal cross section and Gaussian priors for the uncertainties on acceptance and backgrounds. Figure 2 shows the expected and observed limits as a function of $m(\tilde{t}_1)$ for a neutralino mass of 80 GeV/c^2.

We exclude, assuming BR($\tilde{t}_1 \rightarrow c\tilde{\chi}_1^0$) = 100%, $\tilde{t}_1$ masses up to 180 GeV/c^2 at 95% C.L. In addition, a 95% C.L. limit is obtained in the mass parameter plane of the model. Figure 3 shows the excluded region in the stop-neutralino mass plane of the analysis, compared with results from previous analyses [5, 6, 30]. The limit obtained with the present analysis improves the results of previous searches using a similar topology, and repre-
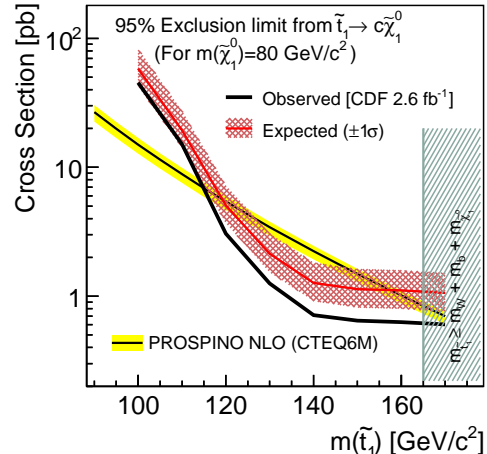

FIG. 2: Observed (solid line) and expected (solid line with dashed band) 95% C.L. upper limit on the stop cross section (solid line with shaded band) as a function of the stop mass for an assumed value of the neutralino mass. The shaded band denotes the uncertainty on the NLO stop pair-production cross section.
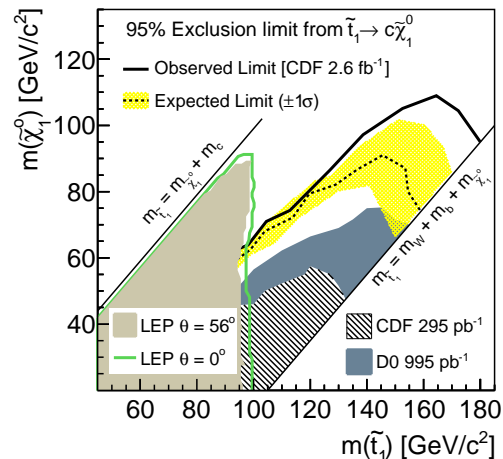

FIG. 3: Excluded region at 95% C.L. in the $m(\tilde{t}_1)$-$m(\tilde{\chi}_1^0)$ plane. The result is compared to the previous results from CDF [5], from D0 [6], and from LEP [30] experiments at CERN.

sents the world's best limit in the region of large mass splitting.

To summarize, we have searched for the pair production of stop decaying into a charm quark and a neutralino, in 2.6 fb^{-1} of CDF Run II data. We observe 115 candidate events, which are in agreement with SM background expectations of 132.0 ± 24.4 events. No evidence for stop is observed, and we exclude a region in the stop and neu-

tralino mass plane at 95% C.L. as shown in Fig. 3. Assuming BR($\tilde{t}_1 \to c\tilde{\chi}_1^0$) = 100%, we exclude stop masses up to 180 GeV/c^2 at 95% C.L. for a neutralino mass of 90 GeV/c^2.

[1] E. Gildener, Phys. Rev. D **14**, 1667 (1976).
[2] For a review of SUSY, see S. P. Martin, hep-ph/9709356, and references therein.
[3] H. Goldberg, Phys. Rev. Lett. **50**, 1419 (1983); J. Ellis *et al.*, Nucl. Phys. **B238** (1984) 453.
[4] A. Bartl, W. Majerotto, and W. Porod, Z. Phys. C **64**, 499 (1994) [Erratum-ibid. C **68**, 518 (1995)].
[5] T. Aaltonen *et al.* (CDF Collaboration), Phys. Rev. D **76**, 072010 (2007).
[6] V.M. Abazov *et al.* (D0 Collaboration), Phys. Lett. B **665**, 1 (2008).
[7] We use a cylindrical coordinate system with its origin at the center of the detector, where θ and ϕ are the polar and azimuthal angles, respectively, and pseudorapidity is $\eta = -\ln(\tan(\frac{\theta}{2}))$. The missing E_T ($\vec{\not{E}}_T$) is defined by $\vec{\not{E}}_T = -\sum_i E_T^i \hat{\mathbf{n}}_\mathbf{i}$, where i = calorimeter tower number and $\hat{\mathbf{n}}_\mathbf{i}$ is a unit vector perpendicular to the beam axis and pointing at the ith calorimeter tower. $\vec{\not{E}}_T$ is corrected for high-energy muons and jet energy. We define $\not{E}_T = |\vec{\not{E}}_T|$. The $\vec{\not{E}}_T^{trk}$ is defined as the negative vector sum of track p_T's requiring tracks with $p_T > 0.5$ GeV. We define $\not{E}_T^{trk} = |\vec{\not{E}}_T^{trk}|$.
[8] D. Acosta *et al.* (CDF Collaboration), Phys. Rev. D **71**, 032001 (2005).
[9] G. Arnison *et al.* (UA1 Collaboration), Phys. Lett. B **123**, 115 (1983); A. Bhatti *et al.*, Nucl. Instrum. Methods A **566**, 375 (2006).
[10] A.Bhatti *et al.* (CDF Collaboration), Nucl. Instrum. Methods A **566**, 375 (2006).
[11] D. Acosta *et al.* (CDF Collaboration), Phys. Rev. D **71**, 052003 (2005).
[12] M. L. Mangano *et al.*, J. High Energy Phys. 07 (2003) 001. We use ALPGEN v. 2.10.
[13] T. Sjöstrand *et al.*, Comput. Phys. Commun. **135**, 238 (2001). We use PYTHIA v. 6.216.
[14] F. Maltoni and T. Stelzer, J. High Energy Phys. 02 (2003) 027. We use MADEVENT v. 4.0.
[15] H. L. Lai *et al.*, Eur. Phys. J. C **12**, 375 (2000).
[16] R. Brun *et al.*, Tech. Rep. CERN-DD/EE/84.1, 1987.
[17] E. Gerchtein and M. Paulini, eConf **C0303241**, TUMT005 (2003).
[18] B. W. Harris *et al.*, Phys. Rev. D **66**, 054024 (2002); Z. Sullivan, Phys. Rev. D **70**, 114012 (2004).
[19] M. Cacciari *et al.*, J. High Energy Phys. 04 (2004) 068.
[20] J. R. Campbell and R. K. Ellis, Phys. Rev. D **60**, 113006 (1999).
[21] J. Campbell and R. K. Ellis, MCFM-Monte Carlo for FeMtobarn processes, http://mcfm.fnal.gov/. We use MCFM v. 5.8.
[22] A. Lister (CDF and D0 Collaborations), arXiv:0810.3350.
[23] T. Aaltonen *et al.* (CDF Collaboration), Phys. Rev. Lett. **102**, 221801(2009).
[24] M. Vidal, Ph.D thesis, CIEMAT, FERMILAB-THESIS-2010-08, 2010.
[25] A. Hocker *et al.*, arXiv:physics/0703039.
[26] W. Beenakker *et al.*, Nucl. Phys. **B492**, 51 (1997); W. Beenakker, R. Hopker, and M. Spira, hep-ph/9611232. We use PROSPINO v. 1.0.
[27] J. Pumplin *et al.*, J. High Energy Phys. 07 (2002) 012.
[28] D. Stump *et al.*, J. High Energy Phys. 10 (2003) 046.
[29] A. Zell *et al.*, http://www.ra.cs.unituebingen.de/SNNS/contact.html.
[30] LEPSUSYWG/04-01.1, http://lepsusy.web.cern.ch/lepsusy/.
[31] J. Heinrich *et al.*, arXiv:physics/0409129.